

A stress model reflecting the effect of the friction angle on rockbursts in coal mines

Jinyang Fan^{1,2}, Jie Chen^{*1}, Deyi Jiang¹, Jianxun Wu^{1,3}, Cai Shu^{**1} and Wei Liu¹

¹State Key Laboratory for the Coal Mine Disaster Dynamics and Controls, Chongqing University, 400044 Chongqing, China

²Université de Nice Sophia-Antipolis, CNRS, Observatoire de la Côte d'Azur, Géoazur, 250 rue Einstein, 06560 Valbonne, France

³Department of Civil, Architectural and Environmental Engineering, The University of Texas at Austin, 78712-0273 Austin Texas, U.S.A.

(Received January 30, 2018, Revised February 25, 2019, Accepted April 16, 2019)

Abstract. Rockburst disasters pose serious threat to mining safety and underground excavation, especially in China, resulting in massive life-wealth loss and even compulsive closed-down of some coal mines. To investigate the mechanism of rockbursts that occur under a state of static forces, a stress model with sidewall as prototype was developed and verified by a group of laboratory experiments and numerical simulations. In this model, roadway sidewall was simplified as a square plate with axial compression and end (horizontal) restraints. The stress field was solved via the Airy stress function. To track the “closeness degree” of the stress state approaching the yield limit, an unbalanced force F was defined based on the Mohr-Coulomb yield criterion. The distribution of the unbalanced force in the plane model indicated that only the friction angle above a critical value could cause the first failure on the coal in the deeper of the sidewall, inducing the occurrence of rockbursts. The laboratory tests reproduced the rockburst process, which was similar to the prediction from the theoretical model, numerical simulation and some disaster scenes.

Keywords: failure; numerical analyses; plasticity; rock; triaxial tests

1. Introduction

Rockbursts are dynamic failures of rock, which poses serious threat to mining safety or underground excavation, especially in China coal mines, resulting in a large amount of casualties and socioeconomic loss (Pan 2009). Even some state-owned coal mines such as Qianqiu coal mine, Henan Province, China, with a production of millions of tons had to be closed down due to continuous occurrence of rockburst. As coal mining depth increases by about 10 m per year, the situation regarding rockburst becomes more and more severe (Cai 2013, Chen *et al.* 2012, Ortlepp and Stacey, 1994). Therefore, research on rockburst mechanism and prediction has become one of the key scientific and technical topic in geomechanics (Song 2017, Li 2016, Fan 2016, 2017). In order to understand rockburst mechanism, scholars have put forward a series of classical theories and models that are useful with a high significance.

Based on source mechanisms, Ortlepp and Stacey (1994) categorized the field rockbursts as: strain bursting, buckling, face crushing, virgin shear in rock mass and reactivated shear on existing faults or discontinuities. Senfaute *et al.* (1997) reported that during a rockburst, the thickness of the ejected rock can be in the order of 1 m and hence supports on the rock must be capable of absorbing the

rock kinetic energy; however, it remained essentially a subject of qualitative study (Feng *et al.* 2011). Lu *et al.* (2012, 2015) and Xu *et al.* (2010) studied rockburst processes under different stress paths in laboratory using the AE monitoring technique and concluded that it may be possible to predict the occurrence of rockburst when a sudden decrease of microseismic rate occurs in one zone while the micro-seismic rate continues to increase in an adjacent zone. He *et al.* (2010) studied the rockburst with true triaxial rock tests system, in which the specimen was loaded in three mutually perpendicular directions and then abrupt unloading of the minimum principal stress in one loading face was performed, creating a stress state and boundary conditions in the rock sample relatively similar to those that exist at a tunnel face. (Dou *et al.* 2014, Li *et al.* 2014) studied the mechanism of structural-instability rockbursts in the region around fault pillar. Their results show that when a coalface approaches a fault area, two or more roof strata simultaneously fracture in the fault area, leading to an increase in the dynamic and static stresses in the pillar, which will then induce the rockburst. These investigations showed that rockburst can be modeled by an abrupt energy release due to variations of the post-peak stiffness of the material.

However, the abrupt energy release as investigated, is almost evoked by artificial rapid unloading/loading, which is discordant with engineering practice: in many cases, as underground excavation and coalface advance progressively, namely, the stress increases gradually, (Bai *et al.* 2015b, Zhang *et al.* 2012) the dead load will take a leading role in triggering rockbursts, especially in future deep coal mine. This work focuses on the evolution of

*Corresponding author, Professor
E-mail: Jiechen023@cqu.edu.cn

**Corresponding author, Lecturer
E-mail: Shucaai@cqu.edu.cn

rockbursts resulting from gradual loading/unloading and the identification of the interrelation between material properties and rockburst. In this paper a stress model for typical rockburst was developed and verified by a group of laboratory experiments and numerical simulations. The results will deepen our understanding of the rockburst mechanism and contribute to the preventive management of rockbursts.

2. Dead stress model for rockburst

Roadway and coalface are places where rockbursts frequently occur. One sidewall of a rectangular roadway (Fig. 1) was selected as prototype for the model because of the similarities in physical configuration. Sidewalls were under axial/vertical compression and end/horizontal restriction by gravity and friction from roof/floor, respectively (Bai *et al.* 2015a, Cai 2013, Zhou and Qian 2013).

2.1 Stress field analysis

This section assumes an isotropic material and a linear elastic constitution before yielding for the model. The end restraint effect is thought of simply as a concentrated load P . In elastic mechanics, a concentrated load can be solved by the Airy stress function.

Airy stress function Φ , which represents the stress state of an arbitrary point A in an infinite plate, can be described as

$$\Phi = \frac{P}{\pi b} r \theta \sin \theta \quad (1)$$

where b is the plate thickness. Each stress component can be solved as shown below

$$\begin{cases} \sigma_r = \frac{1}{r} \frac{\partial \Phi}{\partial r} + \frac{1}{r^2} \frac{\partial^2 \Phi}{\partial \theta^2} = \frac{2P \cos \theta}{\pi b r} \\ \sigma_\theta = \frac{\partial^2 \Phi}{\partial r^2} = 0 \\ \sigma_\theta = -\frac{\partial}{\partial r} \left(\frac{1}{r} \frac{\partial \Phi}{\partial \theta} \right) = 0 \end{cases} \quad (2)$$

The polar coordinates are transformed into Cartesian coordinates. The X, Y direction stress distribution is

$$\begin{cases} \sigma_x = \frac{1}{2} \sigma_r + \frac{1}{2} \sigma_r \cos 2\theta = \sigma_r \cos^2 \theta \\ \sigma_y = \frac{1}{2} \sigma_r - \frac{1}{2} \sigma_r \cos 2\theta = \sigma_r \sin^2 \theta \\ \tau_{xy} = \frac{1}{2} \sigma_r \sin 2\theta = \sigma_r \sin \theta \cos \theta \end{cases} \quad (3)$$

Assuming that the distance between two “ P ” acting point is L and two concentrated loads are the same, the stress (point A) could be written with the superposition principle of elasticity as

$$\begin{cases} \sigma_x = \frac{2P}{\pi b} \left(\frac{\cos^3 \theta_1}{r_1} + \frac{\cos^3 \theta_2}{r_2} \right) \\ \sigma_y = \frac{2P}{\pi b} \left(\frac{\sin \theta_1 \cos^2 \theta_1}{r_1} + \frac{\sin \theta_2 \cos^2 \theta_2}{r_2} \right) \\ \tau_{xy} = \frac{2P}{\pi b} \left(\frac{\sin^2 \theta_1 \cos \theta_1}{r_1} + \frac{\sin^2 \theta_2 \cos \theta_2}{r_2} \right) \end{cases} \quad (4)$$

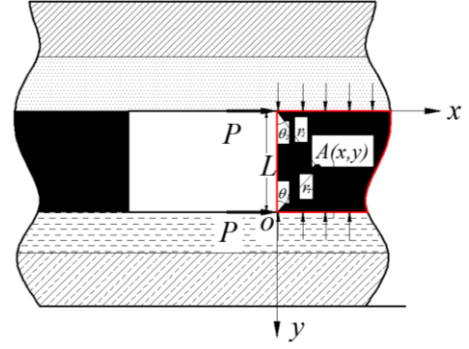


Fig. 1 Diagram of roadway under forces

In Cartesian coordinates, Eq. (4) is expressed as

$$\begin{cases} \sigma_x = \frac{2P}{\pi b} \left(\frac{x^3}{(x^2+y^2)^2} + \frac{x^3}{((L-x)^2+y^2)^2} \right) = \frac{2P}{x\pi b} \left(\frac{x^4}{(x^2+y^2)^2} + \frac{x^4}{((L-x)^2+y^2)^2} \right) \\ \sigma_y = \frac{2P}{\pi b} \left(\frac{xy^2}{(x^2+y^2)^2} + \frac{xy^2}{((L-x)^2+y^2)^2} \right) = \frac{2P}{x\pi b} \left(\frac{x^2y^2}{(x^2+y^2)^2} + \frac{x^2y^2}{((L-x)^2+y^2)^2} \right) \\ \tau_{xy} = \frac{2P}{\pi b} \left(\frac{x^2y}{(x^2+y^2)^2} + \frac{x^2y}{((L-x)^2+y^2)^2} \right) = \frac{2P}{x\pi b} \left(\frac{x^3y}{(x^2+y^2)^2} + \frac{x^3y}{((L-x)^2+y^2)^2} \right) \end{cases} \quad (5)$$

After the excavation of the roadway, the coal mass swells towards the excavation space. Supposing that the roof rock and floor rock are of same characters, the frictions at the contact surface between them and the coal seam are also the same and can be rationally considered to be distributed uniformly. In view of this, we could correct the stress to attempt to match the real condition. We therefore replace $\frac{2P}{x\pi b}$ by a stress coefficient Q . Eq. (5) can be written as

$$\sigma_x = Q \left(\frac{1}{(1+(y/x)^2)^2} + \frac{1}{(1+((L-y)/x)^2)^2} \right) \quad (6)$$

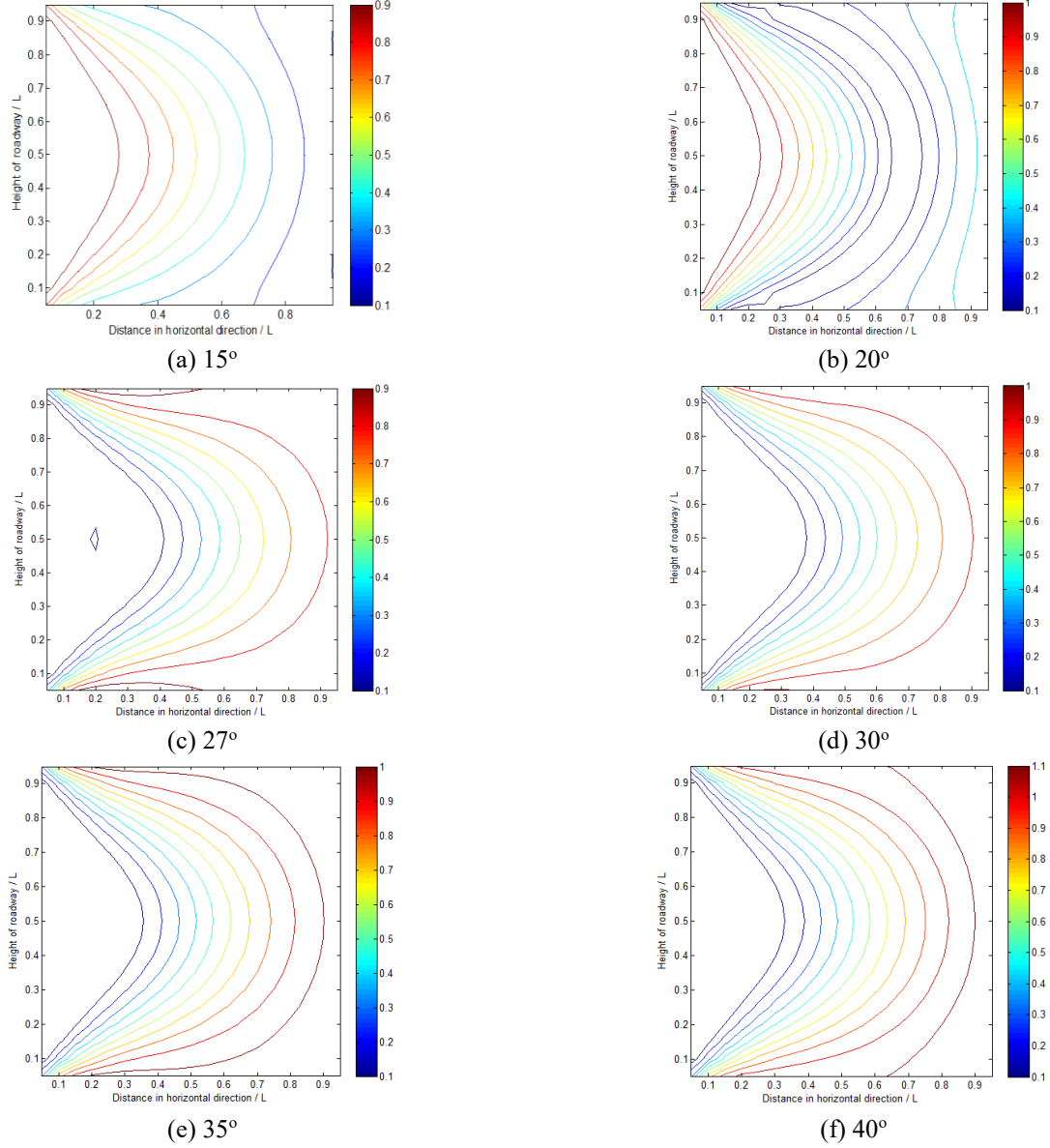
The stress σ_x obtained from Eq. (6) will be used later. In practice, vertical stress σ_y , constitutes complexity. It derives neither from the concentrated load P , nor the overburden load and the stress concentration coefficient (the ratio of maximal vertical stress and situ vertical stress). We define the vertical coefficient C to represent σ_y , and it satisfies the Eq. $\sigma_y = Q \times C$ to keep in a consistent form with σ_x .

$$\sigma_y = Q \times C \quad (7)$$

In mines where rockbursts occur frequently, the measured value of the horizontal pressure ratio K_x (the ratio of situ horizontal stress and situ vertical stress) varies from 1.2 to 2; the measured value of stress concentration coefficient varies from 2 to 4 (Luo 2013, Yong 2015, Yan 2011). From Eq. (6), the range of σ_x can be obtained and is $(0, 2Q)$. According to the underground pressure theory, the stress field after roadway or coal face excavation is composed of a stress growth area, a stress reduction zone and the original rock stress area. Assuming that vertical stress in the stress growth area increases linearly with radial depth, C_{max} could be calculated by the following Eq. (11).

$$C_{max} = 2 \div 1.5 \times 3 \frac{x}{L} = 4 \frac{x}{L} \quad (8)$$

The area of $L \times L$ near the roadway space is selected for analysis. The correction factor is set at 0.6. Usually, on the surface of the sidewall, the vertical stress exists within 0.5-1


 Fig. 2 F value contours with different friction angles, (unit: Q)

time the horizontal stress.

$$\begin{cases} C_{max} = 2 \div 1.5 \times 3 \times 0.6 = 2.4 \\ C_{min} = 0.5 \end{cases} \quad (9)$$

Then,

$$C = 1.9 \frac{x}{L} + 0.5 \quad (10)$$

2.2 Rupture trend analysis

As we know from the failure criterion, no matter what type of rock, the ‘‘closeness degree’’ between real stress and yield limit is an indicator of failure/rupture. Mohr-Coulomb criterion (Alehossein and Poulsen 2010, Bai *et al.* 2015a) is prevalent in geomaterials. The unbalanced force F is defined to tract the ‘‘closeness degree’’ of stress approaching the stress limitation, which is shown as follow

$$F = \sigma_1 - \frac{1 + \sin\varphi}{1 - \sin\varphi} \sigma_3 \quad (11)$$

where σ_1 and σ_3 are the major principal stress and the third principal stress respectively. Substituting Eq. (6), (7) into Eq. (11), we have

$$F = \frac{1 + \sin\varphi}{1 - \sin\varphi} \left(\frac{1}{(1 + (y/x)^2)^2} + \frac{1}{(1 + ((L - y)/x)^2)^2} \right) Q - cQ \quad (12)$$

$$\geq K = 2c_0 \cot\varphi (1 - \sin\varphi)^{-1}$$

where c_0 and φ are the cohesion and the friction angle, respectively. The discriminant factor K can be understood as stress limitation, equal to $2c_0 \cot\varphi (1 - \sin\varphi)^{-1}$. If $F \geq K$, the coal mass will fail. The K is defined by material properties. Replace σ_1 and σ_3 by σ_x , σ_y and τ_{xy}

$$F = \frac{\sigma_x - \sigma_y}{2} + \sqrt{\frac{1}{4}((\sigma_x - \sigma_y)^2 + \tau_{xy}^2)} - \frac{1 + \sin\varphi}{1 - \sin\varphi} \left(\frac{\sigma_x - \sigma_y}{2} - \sqrt{\frac{1}{4}((\sigma_x - \sigma_y)^2 + \tau_{xy}^2)} \right) \quad (13)$$

Eq. (13) can be simplified

$$F = \frac{1 + \sin\varphi}{1 - \sin\varphi} \sigma_x - \sigma_y \geq K = 2c_o \cot\varphi (1 - \sin\varphi)^{-1} \quad (14)$$

Substituting Eq. (10) into Eq. (14) and setting φ at 15° , F contours could be obtained with Matlab (Fig. 2a). With changeable friction angles (20° , 27° , 30° , 35° , 40°), new distributions of F values were shown in Fig. 2b, 2c, 2d, 2e, 2f, respectively. With a friction angle below 27° , the maximal F contour appears on the left of the model, that is, the shallow of the sidewall or workface and F value has a decreasing tendency from the shallow to the deep. That suggests that the sidewall coal failure forms from the shallow to the deep, i.e., the elastic energy which accumulates inside the rock mass could be released gradually with the progressive failure. However, when the friction angle φ is above 27° (including 27°), the F value increases in the horizontal direction from left to right and the maximal F contour appears in the deep of the coal. That means the failure initiates in the deep. If the deep coal fails and attempts to dilate toward the roadway space, the shallow rock has to be unavoidably extruded out, thus, inducing a sudden and collective energy release from the shallower and deeper zones. As a result, the rock bursts out and the fragments are ejected. Therefore, the friction angle is critical to rockburst disasters. The value above which the coal failure initiates in the deeper zone is called critical friction angle.

Additionally, the depth of the maximal F value increases with the friction angle φ , which indicates that a larger friction angle, a deeper failure initiation and a stronger energy release will induce more damage. On the other hand, the cohesion c_o and the friction angle φ are the key components of the discriminant factor K . As known from Eq. (14), larger cohesion connotes a higher/stronger discriminant factor. To some degree it can prevent rockburst occurrence or just defer the rockburst when the crustal stress is high enough; once rockburst takes place, greater harm will be inflicted to the underground construction. Therefore, the friction angle φ is the pivotal factor to decide the occurrence. However the friction angle φ and the cohesion c_o collectively influence the destructive power of rockburst.

3. Laboratory rockburst experiments and numerical simulation

3.1 Experimental conditions

Samples were collected from the Pingdingshan Tian'an Coal Mine, Henan Province, China, where rockburst accidents occurred many times. The mine coal's properties are shown in Table 1. Coal samples were shaped into $\Phi 50$ mm cylindrical blocks with 50 mm height (h) (see Fig. 3). The evenness of head faces was controlled within 0.02 mm; the loading rate was set at 0.2 mm/min. A fixed steel hoop was applied at each end to limit the deformation. Coal samples were compressed under the standard uniaxial compression experimental procedure.

3.2 Failure characteristics of bump-prone coal

Fig. 4 shows the rupture process of samples with end



Fig. 3 Processed samples

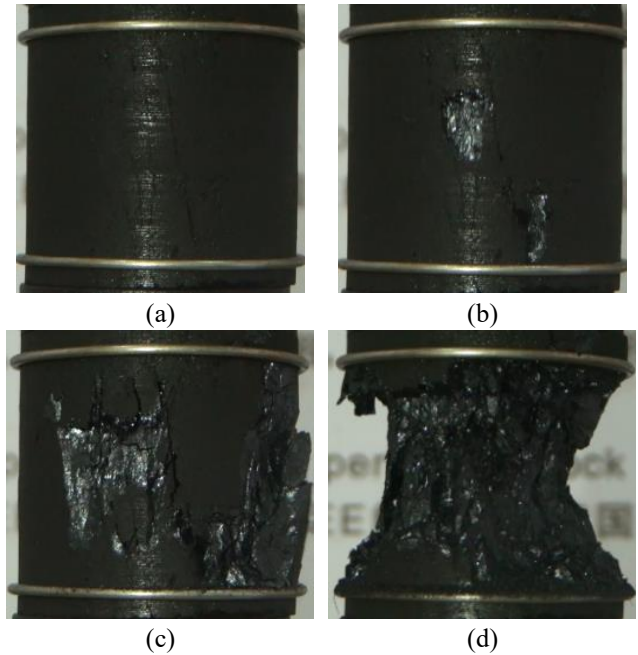


Fig. 4 Failure process of coal samples

constraints. Under the “protection” effect of the hoops, the samples displayed a triangle rupture surface which finally appeared all over the samples surfaces (Fig. 4(d)) and reflected the shape of F contours. Moreover, He *et al.*, obtained a similar concave surface of fracture for limestone, mudstone and peridotite but by a stimulation process using immediate unloading of σ_3 in ture 3-D tests (Cai 2013, He *et al.* 2012c, 2010). We also conducted a series of experiments on weak/soft coal samples, which had 12° friction angle, under the same conditions. There was an apparent abrupt failure during the experiments. In the presented experiment, obvious rockburst phenomena were observed.

Based on the rupture process of coal in the present experiments, the structural integrity instability of coal exhibited stage features. ① When the stress was small, there was no significant change on the coal (Fig. 4(a)). The first burst phenomenon appeared on the surface of the sample (Fig. 4b) at around 60% of the peak strength. There were some visible fragment ejections accompanied by a crackling sound; however, the amount of coal shooting off was very small. ② When the stress reached approximately 78% of the peak strength, the second burst phenomenon appeared (Fig. 4(c)), again accompanied by a crackling

Table 1 Properties of coal from rock-burst-mine

Coal Mine	Density (Kg/m ³)	Compressive strength (MPa)	Tensile strength (MPa)	Cohesion (MPa)	Friction angle (°)	Elasticity modulus (GPa)	Poisson rate	Mining Area
Xinzhouyao Coal Mine	1220	26	2.6	5.11	29.5	--	--	Datong Zone
Tongjialiang Coal Mine	1260	14.5	2.31	3.53	27.4	--	--	Datong Zone
Meiyukou Coal Mine	1260	23.9	3.2	3.07	28.4	--	--	Datong Zone
Chengshan Coal Mine	--	13.98	0.98	--	--	2.67	0.2	Jixi Zone
Qianqiu Coal Mine	1440	19.45	0.7	5.10	34.7	3.83	0.15	Yima Zone
Tian'an Coal Mine	1600	12.92	1.27	4.81	27	2.12	0.21	Pingdingshan Zone

Table 2 Parameters of surrounding materials

Surrounding rock	Density (Kg/m ³)	Compressive strength (MPa)	Tensile strength (MPa)	Cohesion (MPa)	Friction angle (°)	Elasticity modulus (GPa)	Poisson rate
Roof rock	2550	84.13	5.76	5.53	33	19.95	0.16
Coal seam	1600	12.92	1.27	4.81	27	2.12	0.21
Floor rock	2550	84.13	5.76	5.53	33	19.95	0.16

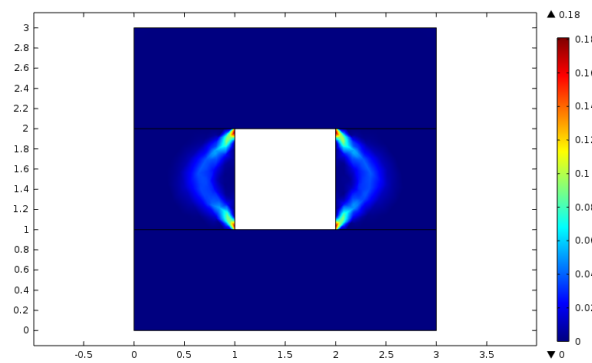


Fig. 5 Roadway stress and plastic strain distribution nephogram



(a) Datong Xinzhou mine, Shanxi, China



(b) Yima Yuejin mine, Henan, China

Fig. 6 Photos from rock burst scenes

sound. This time, the amount of coal was much larger than the previous. Then, there was another silence period. ③ When the stress almost reached the peak strength, a large amount of coal was sharply extruded out (Fig. 4(d)) and the stress dropped dramatically to a lower level.

Compared with the previous two, the ejection and concomitant noise of the third are the strongest. As

described by some scientists, the first two times of ejection could correspond to some coal/rock portentous extrusion before the rockburst; the last strongest one marked the real burst. Judging from the field scene (Fig. 5), the concave triangular surface forming after the disaster is similar with the surface of the samples after the experiments. Therefore, the result from our tests can imply that the stress state built in our model is reasonable to a certain extent.

The properties of coal in mines where the rockbursts often took place (Luo 2013, Yong 2015, Yan 2011), were listed in Table 1, showing that all of the coal in rockburst-mines have a large friction angle above the critical friction angle 27° (including 27°). Note that this model is established, based on the linear distribution of vertical stress as described previously. In practice, the stress configuration is extremely complicated and depends on the geology and the lithology. The critical friction angle will also change for different environments.

3.3 Numerical stimulation

Based on the model, it can be predicted that the plastic area would initiate along with the maximum F contour. In this section, the prediction is verified by numerical stimulation. If the coal mass and the surrounding rock mass obey the Mohr-Coulomb yield criterion (Alehossein and Poulsen 2010, Bai *et al.* 2015a), based on that criterion and the Prandtl-Reuss incremental rule, the plastic strain field could be calculated with COMSOL Multiphysics 4.4 computing platform.

The material parameters values of the relevant seam were also taken, in accordance with the conditions of the Pingdingshan Tian'an Coal Mine (listed in Table 2). The boundary conditions were assigned as follows: two lateral faces were sliding constraint surfaces; the bottom face was a fixed displacement constraint surface while the upper face was a free surface subjected to a vertical pressure (20 MPa). The model dimension was set to 6×6 m (the thickness of coal seam is 2 m). Fig. 5 shows the plastic strain distribution nephogram, in which the red color represents a higher plastic strain. The following plasticity characteristics were observed: ① compared with other areas, plastic strain at the corner was very large because of the stress concentration, which generated during the load charges around the corners of roadways, due to the different mechanical responses from proof and floor rocks and coal; ② the static distribution of the plastic strain band appeared triangular, which is coherent with the results obtained by the theoretical model established in Section 2; ③ the elastic-plastic boundary was similar with the F value contour. The results of the simulation are also similar with the picture taken from the disaster scene (Fig. 6).

4. Conclusions

To facilitate the analysis, one typical area in the coal mine was selected and reasonably simplified for rockburst. By the Airy stress function, we obtained the stress field. Based on the Mohr-Coulomb criterion and the definition of the unbalanced force, the friction angle was found to be a critical factor determining the potential of rockburst. When the friction angle is small, the maximum unbalanced force appears in the shallow sidewall of coal seam, resulting in a progressive failure and a smooth energy release. This could hardly lead to rockburst. As the friction angle goes beyond the critical value, the maximum unbalanced force appears in

the deep. The failure therefore initiates in the deep. If the deep coal fails and attempts to spread towards the roadway space, the shallow rock has to be unavoidably extruded out, thus, inducing a sudden energy release. As a result, the rock bursts out and fragments are ejected.

Laboratory experiments and numerical simulations provided coherent results with the theoretical prediction. During the tests, the rockburst was stimulated using the bump-prone coal under a similar stress state to the model. There were three stages observed during rockburst: the early two portentous ejections and the last real rockburst.

Acknowledgements

This work was supported by the National Key R&D Program of China (2017YFC0804202), the National Natural Science Fund (No. 51834003, 41672292, 51574048), China Postdoctoral Science Foundation (2018M633318), the Fundamental Research Funds for the Central Universities (No. 2018CDQYZH0018), which are all greatly appreciated.

References

- Alehossein, H. and Poulsen, B.A. (2010), "Stress analysis of longwall top coal caving", *Int. J. Rock Mech. Min. Sci.*, **47**(1), 30-41. <https://doi.org/10.1016/j.ijrmms.2009.07.004>.
- Bai, H., Li, W., Ding, Q., Wang, Q. and Yang, D. (2015a), "Interaction mechanism of the interface between a deep buried sand and a paleo-weathered rock mass using a high normal stress direct shear apparatus", *Int. J. Min. Sci. Technol.*, **25**(4), 623-628. <https://doi.org/10.1016/j.ijmst.2015.05.016>.
- Bai, Q., Tu, S., Li, Z. and Tu, H. (2015b), "Theoretical analysis on the deformation characteristics of coal wall in a longwall top coal caving face", *Int. J. Min. Sci. Technol.*, **25**(2), 199-204. <https://doi.org/10.1016/j.ijmst.2015.02.006>.
- Cai, M. (2013), "Principles of rock support in burst-prone ground", *Tunn. Undergr. Sp. Technol.*, **36**, 46-56. <https://doi.org/10.1016/j.tust.2013.02.003>.
- Chen, X., Li, W. and Yan, X. (2012), "Analysis on rock burst danger when fully-mechanized caving coal face passed fault with deep mining", *Safety Sci.*, **50**(4), 645-648. <https://doi.org/10.1016/j.ssci.2011.08.063>.
- Dou, L.M., He, X.Q., Hu, H.E., He, J. and Fan, J. (2014), "Spatial structure evolution of overlying strata and inducing mechanism of rockburst in coal mine", *Trans. Nonferr. Metals Soc. China*, **24**(4), 1255-1261. [https://doi.org/10.1016/S1003-6326\(14\)63187-3](https://doi.org/10.1016/S1003-6326(14)63187-3).
- Driad-Lebeau, L., Lahaie, F., Al Heib, M., Josien, J.P., Bigarré, P. and Noirel, J.F. (2005), "Seismic and geotechnical investigations following a rockburst in a complex French mining district", *Int. J. Coal Geol.*, **64**(1-2), 66-78. <https://doi.org/10.1016/j.coal.2005.03.017>.
- Fan, J., Chen, J., Jiang D., Chemenda A., Chen J. and Ambre J. (2017), "Discontinuous cyclic loading test with acoustic emission monitoring", *Int. J. Fatigue*, **94**(1), 140-144. <https://doi.org/10.1016/j.ijfatigue.2016.09.016>.
- Fan, J., Chen, J., Jiang D., Ren S. and Wu J. (2016), "Fatigue properties of rock salt subjected to interval cyclic pressure", *Int. J. Fatigue*, **90**(9), 109-115. <https://doi.org/10.1016/j.ijfatigue.2016.04.021>.
- Fan, J., Dou, L., He, H., Du, T., Zhang, S., Gui, B. and Sun, X. (2012), "Directional hydraulic fracturing to control hard-roof

- rockburst in coal mine”, *Int. J. Min. Sci. Technol.*, **22**(2), 177-181. <https://doi.org/10.1016/j.ijmst.2011.08.007>.
- Feng, X., Wang, E., Shen, R., Wei, M., Yu, C. and Cao, X. (2011), “The dynamic impact of rock burst induced by the fracture of the thick and hard key stratum”, *Procedia Eng.*, **26**, 457-465. <https://doi.org/10.1016/j.proeng.2011.11.2192>.
- Frid, V. (1997), “Rockburst hazard forecast by electromagnetic radiation excited by rock fracture”, *Rock Mech. Rock Eng.*, **30**(4), 229-236. <https://doi.org/10.1007/BF01045719>.
- Fujii, Y., Ishijima, Y. and Deguchi, G. (1997), “Prediction of coal face rockbursts and microseismicity in deep longwall coal mining”, *Int. J. Rock Mech. Min. Sci.*, **34**(1), 85-96. [https://doi.org/10.1016/S1365-1609\(97\)80035-4](https://doi.org/10.1016/S1365-1609(97)80035-4).
- He, H., Dou, L., Fan, J., Du, T. and Sun, X. (2012a), “Deep-hole directional fracturing of thick hard roof for rockburst prevention”, *Tunn. Undergr. Sp. Technol.*, **32**, 34-43. <https://doi.org/10.1016/j.tust.2012.05.002>.
- He, J., Dou, L.M., Cao, A.Y., Gong, S.Y. and Lü, J.W. (2012b), “Rock burst induced by roof breakage and its prevention”, *J. Central South Univ.*, **19**(4), 1086-1091. <https://doi.org/10.1007/s11771-012-1113-3>.
- He, M., Xia, H., Jia, X., Gong, W., Zhao, F. and Liang, K. (2012c), “Studies on classification, criteria and control of rockbursts”, *J. Rock Mech. Geotech. Eng.*, **4**(2), 97-114. <https://doi.org/10.3724/SP.J.1235.2012.00097>.
- He, M.C., Miao, J.L. and Feng, J.L. (2010), “Rock burst process of limestone and its acoustic emission characteristics under true-triaxial unloading conditions”, *Int. J. Rock Mech. Min. Sci.*, **47**(2), 286-298. <https://doi.org/10.1016/j.ijrmms.2009.09.003>.
- Konicek, P., Soucek, K., Stas, L. and Singh, R. (2013), “Long-hole destress blasting for rockburst control during deep underground coal mining”, *Int. J. Rock Mech. Min. Sci.*, **61**, 141-153. <https://doi.org/10.1016/j.ijrmms.2013.02.001>.
- Leśniak, A. and Isakow, Z. (2009), “Space-time clustering of seismic events and hazard assessment in the Zabrze-Bielszowice coal mine, Poland”, *Int. J. Rock Mech. Min. Sci.*, **46**(5), 918-928. <https://doi.org/10.1016/j.ijrmms.2008.12.003>.
- Li, X., Wang, E., Li, Z., Bie, X., Chen, L., Feng, J. and Li, N. (2016), “Blasting wave pattern recognition based on Hilbert-Huang transform”, *Geomech. Eng.*, **11**(5), 607-624. <https://doi.org/10.12989/gae.2016.11.5.607>.
- Li, Z., Dou, L., Cai, W., Wang, G., He, J., Gong, S. and Ding, Y. (2014), “Investigation and analysis of the rock burst mechanism induced within fault-pillars”, *Int. J. Rock Mech. Min. Sci.*, **70**, 192-200. <https://doi.org/10.1016/j.ijrmms.2014.03.014>.
- Lu, A.H., Mao, X.B. and Liu, H.S. (2008), “Physical simulation of rock burst induced by stress waves”, *J. China Univ. Min. Technol.*, **18**(3), 401-405. [https://doi.org/10.1016/S1006-1266\(08\)60084-X](https://doi.org/10.1016/S1006-1266(08)60084-X).
- Lu, C.P., Dou, L.M., Liu, B., Xie, Y.S. and Liu, H.S. (2012), “Microseismic low-frequency precursor effect of bursting failure of coal and rock”, *J. Appl. Geophys.*, **79**, 55-63. <https://doi.org/10.1016/j.jappgeo.2011.12.013>.
- Lu, C.P., Liu, G.J., Liu, Y., Zhang, N., Xue, J.H. and Zhang, L. (2015), “Microseismic multi-parameter characteristics of rockburst hazard induced by hard roof fall and high stress concentration”, *Int. J. Rock Mech. Min. Sci.*, **76**, 18-32. <https://doi.org/10.1016/j.ijrmms.2015.02.005>.
- Luo, J. (2013), “Research on the mechanism of rock burst in coal roadway under extremely thick igneous rocks and control techniques”, China University of Mining and Technology, Xuzhou, China.
- Ning, J., Wang, J., Liu, X., Qian, K. and Sun, B. (2014), “Soft-strong supporting mechanism of gob-side entry retaining in deep coal seams threatened by rockburst”, *Int. J. Min. Sci. Technol.*, **24**(6), 805-810. <https://doi.org/10.1016/j.ijmst.2014.10.012>.
- Ortlepp, W.D. and Stacey, T.R. (1994), “Rockburst mechanisms in tunnels and shafts”, *Tunn. Undergr. Sp. Technol.*, **9**(1), 59-65. [https://doi.org/10.1016/0886-7798\(94\)90010-8](https://doi.org/10.1016/0886-7798(94)90010-8).
- Pan, J., Meng, Z., Hou, Q., Ju, Y. and Li, G. (2009), “Influence of the roof lithological characteristics on rock burst: A case study in Tangshan colliery, China”, *Geomech. Eng.*, **1**(2), 143-154. <https://doi.org/10.12989/gae.2009.1.2.143>.
- Senfaute, G., Chambon, C., Bigarré, P., Guise, Y. and Josien, P.J. (1997), “Spatial distribution of mining tremors and the relationship to rockburst hazard”, *Pure Appl. Geophys.*, **150**(3), 451-459. <https://doi.org/10.1007/s000240050087>.
- Song, D., Wang, E., Li, Z., Qiu, L. and Xu, Z. (2017), “An effective method for monitoring and warning of rock burst hazard”, *Geomech. Eng.*, **12**(1), 53-69. <https://doi.org/10.12989/gae.2017.12.1.53>.
- Taupin, V., Berbenni, S., Fressengeas, C. and Bouaziz, O. (2010), “On particle size effects: An internal length mean field approach using field dislocation mechanics”, *Acta Materialia*, **58**(16), 5532-5544. <https://doi.org/10.1016/j.actamat.2010.06.034>.
- Tsirel, S.V. and Krotov, N.V. (2001), “Probability interpretation of indirect risk criteria and estimate of rock-burst hazard in mining anthracite seams”, *J. Min. Sci.*, **37**(3), 240-260. <https://doi.org/10.1023/A:1013194110443>.
- Wang, L., Lu, Z. and Gao, Q. (2012), “A numerical study of rock burst development and strain energy release”, *Int. J. Min. Sci. Technol.*, **22**(5), 675-680. <https://doi.org/10.1016/j.ijmst.2012.08.014>.
- Xu, X., Dou, L., Lu, C. and Zhang, Y. (2010), “Frequency spectrum analysis on micro-seismic signal of rock bursts induced by dynamic disturbance”, *Min. Sci. Technol.*, **20**(5), 682-685. [https://doi.org/10.1016/S1674-5264\(09\)60262-3](https://doi.org/10.1016/S1674-5264(09)60262-3).
- Yan, Y. (2011), “Research on the mechanism and technology of rock burst control in Datong coal mining area”, Taiyuan University of Technology, Taiyuan, China.
- Yong, L. (2015), “Study of mechanism and control of coal bumps in JIXI mine area”, China University of Mining and Technology, Xuzhou, China.
- Zhang, R.L., Wang, Z.J. and Chen, J.W. (2012), “Experimental research on the variational characteristics of vertical stress of soft coal seam in front of mining face”, *Safety Sci.*, **50**(4), 723-727. <https://doi.org/10.1016/j.ssci.2011.08.045>.
- Zhang, X. and Aifantis, K.E. (2015), “Examining the evolution of the internal length as a function of plastic strain”, *Mater. Sci. Eng. A*, **631**, 27-32. <https://doi.org/10.1016/j.msea.2015.01.011>.
- Zhao, Y. and Jiang, Y. (2010), “Acoustic emission and thermal infrared precursors associated with bump-prone coal failure”, *Int. J. Coal Geol.*, **83**(1), 11-20. <https://doi.org/10.1016/j.coal.2010.04.001>.
- Zhou, X. and Qian, Q. (2013), “The non-Euclidean model of failure of the deep rock masses under the deformation incompatibility condition”, *J. Min. Sci.*, **49**(3), 368-375. <https://doi.org/10.1134/S1062739149030039>.
- Zhou, X.P., Qian, Q.H. and Yang, H.Q. (2011), “Rock burst of deep circular tunnels surrounded by weakened rock mass with cracks”, *Theor. Appl. Fract. Mech.*, **56**(2), 79-88. <https://doi.org/10.1016/j.tafmec.2011.10.003>.